

A microfluidic refractive index sensor based on an integrated three-dimensional photonic crystal

Jing Wu, Daniel Day,^{a)} and Min Gu

Centre for Micro-Photonics, Faculty of Engineering and Industrial Sciences, Swinburne University of Technology, P.O. BOX 218, Victoria 3122, Australia

(Received 5 December 2007; accepted 16 January 2008; published online 20 February 2008)

We present the concept of using three-dimensional photonic crystals for refractive index sensing in a microfluidic channel. The sensors are based on a three-dimensional void channel photonic crystal fabricated by femtosecond laser writing in a polymer substrate. It is demonstrated that a change in the refractive index of the fluid in the microchannel results in a shift in the band gap or band gap defect position of the photonic crystal. According to Fourier transform infrared spectroscopy of the photonic crystal sensor, a change of 6×10^{-3} in the refractive index of the fluid can be detected.

© 2008 American Institute of Physics. [DOI: 10.1063/1.2840700]

Microfluidics has received an increasing amount of attention since the 1990s, as it is rapidly transforming the way with which biological, chemical, and physical researches are being conducted. The continued development of functional micrototal-analysis systems (μ TAS) or lab-on-a-chip devices for processes such as high-throughput screening, clinical analysis or biochemical synthesis will ultimately require the integration of sensing elements for detection and analysis. Integrated optical sensors are capable of achieving high sensitivity and high throughput with independent noncontact sensing techniques using either labeled or label-free protocols. While the range of optical sensing technologies compatible with microfluidic devices are based on methods such as absorbance, fluorescence or surface-plasmon-resonance, it is the ability to detect changes in refractive index associated with the binding of biomaterials that is generating significant interest due to the potential to monitor biochemical reactions without the need for fluorescently tag molecules.^{1,2}

Photonic crystal structures have recently been demonstrated as optical biosensors.^{3,4} Due to the highly localized confinement of the coupled light, photonic crystal sensors can be incorporated into microfluidic devices to facilitate localized measurements of the change in refractive index. To date, most of the research with photonic crystal sensors in microfluidic devices have been limited to one-dimensional or two-dimensional photonic crystal sensors.⁵ At present the only three-dimensional (3D) photonic crystals used for biosensing have been fabricated by self-assembly.⁶ Three-dimensional photonic crystals based on the woodpile geometry or face-centered-tetragonal lattice (fct) have been an active research topic not only because of the ability of opening up a complete band gap but also of their great flexibility in tuning the photonic band gap effect by manipulating the geometrical parameters through the fabrication parameters (scanning speed, laser power, laser wavelength, or pulse duration).⁷

Here, we present an integrated 3D photonic crystal microfluidic sensor fabricated with a femtosecond laser. In this work, a 3D photonic crystal microfluidic sensor based on femtosecond laser fabricated void channels in a polymer sub-

strate is used. When the 3D photonic crystal sensor is integrated with a microfluidic channel, a shift in the band gap and band gap defect peak positions are observed according to changes, in the refractive index of the fluid.

The sensor and microfluidic channel are fabricated in two steps using femtosecond laser direct writing. First, a 3D photonic crystal based on void channels is fabricated in a precured Norland optical adhesive (NOA 63) polymer substrate (Norland Inc.). The laser beam (810 nm) from a femtosecond laser pumps an optical parameter oscillator operating at 580 nm (76 MHz, 200 fs). The beam is then expanded and collimated to uniformly illuminate the back aperture of an Olympus PlanApo 1.4 numerical aperture (NA) oil immersion objective and then focused into the precured polymer substrate. The laser power used to create void channels is 32 mW with a sample translation speed of 450 $\mu\text{m/s}$. In the second process, a microfluidic channel is fabricated by etching a channel in the polymer substrate with an amplified femtosecond laser beam (800 nm, 1 kHz, 110 fs) focused through a 0.25 NA objective lens. The fabrication energy is 15 μJ per pulse with a sample translation speed of 1500 $\mu\text{m/s}$. By scanning the amplified beam across the polymer substrate, a microchannel can be etched into the surface directly above the photonic crystal. After the fabrication of the 3D photonic crystals and microfluidic channels, the channels were sealed with a layer of polydimethylsiloxane (PDMS) polymer. The PDMS was prepared by spin coating at 1200 rpm on a glass slide and cured at 75 °C for 20 min, after which it was transferred to the microfluidic polymer substrate. Polydimethylsiloxane was chosen because of its good elasticity, optical transparency, and biocompatibility. An illustration of the sensor is shown in Fig. 1(a) and a scanning electron microscope (SEM) image of the etched channel above the sensor is shown in Fig. 1(b). The distance separating the photonic crystal and the microfluidic channel is less than 10 μm . Refractive index fluids (Cargille Laboratories, USA) were introduced into one end of the microfluidic channel, with capillary force drawing the fluid into the remainder of the channel. After each optical measurement a washing procedure was used to rinse the channel before introducing another refractive index fluid. The response of the photonic crystal microfluidic sensors were characterized with Fourier transform infrared (FTIR) spec-

^{a)} Author to whom correspondence should be addressed. Electronic mail: dday@swin.edu.au.

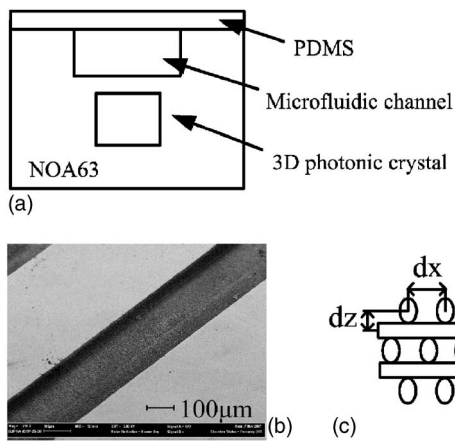


FIG. 1. (a) A schematic diagram of the integrated 3D photonic crystal microfluidic sensor. (b) A SEM image of etched femtosecond laser etched microchannel above the photonic crystal and (c) an illustration of the unit cell for the woodpile photonic crystal structure, where δz and δx are the layer spacing and in-plane spacing, respectively.

troscopy. The infrared spectra of the photonic crystal structures were measured using a Nicolet Nexus Fourier transform infrared spectrometer with a Continuum infrared microscope ($32\times$ NA 0.65 objective and condenser).

In our experiments, 24 layer woodpile photonic crystals, without and with a planar defect, were fabricated.⁸ The range of the physical parameters for the woodpile photonic crystals are $\delta x=1.3\text{--}1.4\ \mu\text{m}$ for the in-plane spacing and $\delta z=1.4\text{--}1.5\ \mu\text{m}$ for the layer spacing. An illustration of the unit cell is shown in Fig. 1(c), respectively. For the photonic crystal with a planar defect, the 13th through 24th layers are displaced by a distance $\Delta d=0.3\ \mu\text{m}$, creating a microcavity defect between the 12th and 13th layers of the photonic crystal, resulting in a Fabry-Pérot (FP) cavity. The properties of the planar defect can be tailored in order to produce a FP resonance peak in the photonic crystal band gap.⁸

Figure 2 demonstrates that photonic crystals can be integrated into a microfluidic device without negatively affecting the performance of the photonic crystal. A photonic band gap with a suppression of the infrared transmission of 85% in the stacking direction can still be achieved [see Fig. 2(a)]

for a 3D woodpile photonic crystal. The photonic crystal is a 24 layer woodpile void channel structure with a layer spacing $\delta z=1.5\ \mu\text{m}$ and an in-plane spacing $\delta x=1.3\ \mu\text{m}$, as shown in Fig. 2(b). The experimentally measured photonic band gap of the microfluidic photonic crystal sensor corresponds quite well with the theoretically predicted band calculation along the stacking direction of $\Gamma\text{-X}'$, shown in Fig. 2(c). The center of the stop gap in Fig. 2(c) is located at a frequency of 0.2981 which correlates to a wavelength of $4.693\ \mu\text{m}$ that is consistent with the experimentally measured band gap. For the photonic crystal with a planar defect, the suppression of the infrared transmission of 80% is achieved with a FP resonance peak positioned in the middle of the band gap [see Fig. 2(d)]. The photonic crystal with a planar defect is a 24 layer woodpile void channel structure with a layer spacing $\delta z=1.5\ \mu\text{m}$, an in-plane spacing $\delta x=1.4\ \mu\text{m}$ and a defect spacing of $\Delta d=0.3\ \mu\text{m}$, as illustrated in Fig. 2(e). The FP resonance peak is located at a frequency of 0.315 which corresponds to a wavelength of $4.441\ \mu\text{m}$. The experimental measurements of the band gap and defect are again confirmed by the theoretical band calculations along the $\Gamma\text{-X}'$ direction, as shown in Fig. 2(f). The agreement between the experimental measurements and theoretical predictions of the band gap confirms that the photonic crystal and microfluidic channel can be integrated into a single piece of polymer substrate. Figure 2 also demonstrates that the surface roughness produced by the laser machining of the channel does not affect the performance of the photonic crystal.

To demonstrate the ability of the 3D photonic crystal to sense changes in refractive index, a series of index matching fluids were introduced into the microfluidic channel. Figure 3(a) shows the measured position of the photonic band gap as a function of the index of refraction of the liquid in the microchannel. The photonic crystal is a 24 layer woodpile void channel structure with a layer spacing $\delta z=1.5\ \mu\text{m}$ and an in-plane spacing $\delta x=1.3\ \mu\text{m}$. As the index of refraction of the liquid is increased, a linear shift in the band gap position to longer wavelengths is recorded. A shift in the photonic band gap of 35 nm is measured for a change in refractive index of the liquid of $\Delta n=0.3$, which corresponds to a

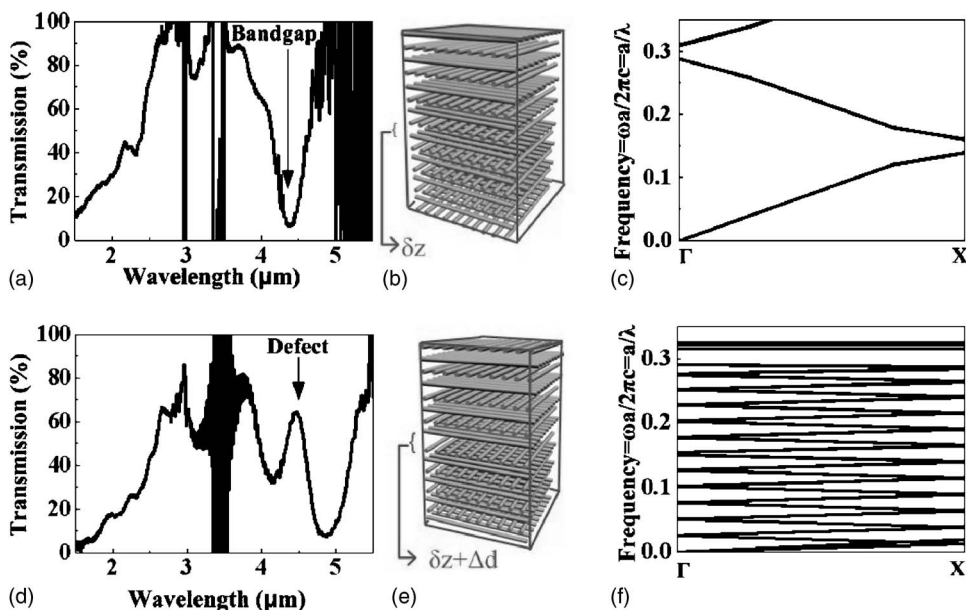


FIG. 2. (a) FTIR spectrum of the integrated 24 layer photonic crystal sensor with $\delta z=1.5\ \mu\text{m}$ and $\delta x=1.3\ \mu\text{m}$. The photonic band gap in the stacking direction produces an 85% suppression of the infrared transmission at $4.693\ \mu\text{m}$ and (b) an illustration of the 24 layer photonic crystal structure. (c) Photonic band structure calculation for the photonic crystal showing the photonic band gap at the normalized frequency of 0.2981. (d) FTIR spectrum of the integrated 24 layer photonic crystal sensor with $\delta z=1.5\ \mu\text{m}$, $\delta x=1.3\ \mu\text{m}$, and $\Delta d=0.3\ \mu\text{m}$. The planar defect results in a FP resonance peak at $4.441\ \mu\text{m}$ and (e) an illustration of the photonic crystal with a planar defect between the 12th and 13th layers. (f) The photonic band structure calculation showing the band gap and defect resonance located at the normalized frequency of 0.315.

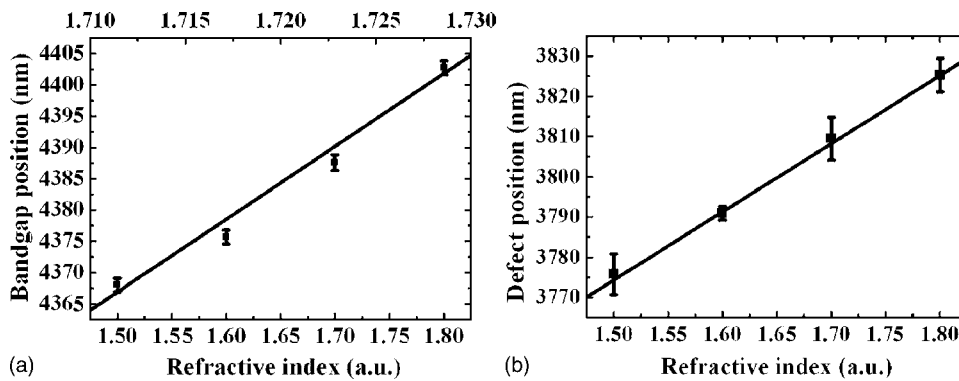


FIG. 3. The shift in the position of the photonic band gap (a) and defect resonance (b) as the index of refraction of the liquid in the microchannel is increased. The averaged refractive index of the photonic crystal sensor according to Eq. (1) is displayed on the secondary x axis.

sensitivity of 8×10^{-3} in refractive index. The sensitivity of the sensor is defined as the detectable change in refractive index of the fluid as a function of the photonic band gap shift ($\Delta n/\Delta \lambda$) in the FTIR spectrum of the photonic crystal. The resolution of the minimum detectable wavelength shift of the band gap of 1 nm has been determined which is limited by the width of the photonic band gap and the accuracy of the FTIR for the region where the band gap appears. The measurements of the band gap position as a function of the refractive index of the liquid is displayed in Fig. 3(a) as the average of three repeated experiments with the error bars representing the variation of the measured value. The sensitivity of the 3D photonic crystal is an improvement on the published two-dimensional photonic crystal sensor which demonstrated a sensitivity of 1×10^{-2} .⁵ To determine the band gap position as a function of the average refractive index of the sensor and photonic crystal geometrical parameters, we can interpret the change in average refractive index (n_{avg}) of the photonic crystal sensor based on the change in position of the band gap, given by⁹

$$m\lambda_{\text{gap}} \approx 2\delta z n_{\text{avg}} \approx 2\delta z [n - A/(\delta z \delta x)(n - 1)], \quad (1)$$

where λ_{gap} is the band gap position, A is the cross section of the void channel, and n is the effective refractive index of the polymer material. The average refractive index of the photonic crystal sensor is displayed on the secondary x axis (top of the frame) in Fig. 3(a). As the relationship between the average refractive index and the position of the band gap is known, this sensor can be used to determine the absolute value of the refractive index rather than a relative value to within an accuracy of 8×10^{-3} .

As the photonic band gap can be relatively broad with respect to the change in position of the band gap, a photonic crystal with a planar defect was fabricated in order to utilize the resulting FP cavity resonance. The position and finesse of the FP cavity can be tuned by the geometrical properties of the photonic crystal and planar defect. Figure 3(b) shows the measured position of the FP resonance as the refractive index of the liquid in the microchannel is changed. The photonic crystal with a planar defect is a 24 layer woodpile void chan-

nel structure with a layer spacing $\delta z = 1.4 \mu\text{m}$, an in-plane spacing $\delta x = 1.3 \mu\text{m}$, and a defect spacing of $\Delta d = 0.3 \mu\text{m}$. The measurements of the band gap position as a function of the refractive index of the liquid is displayed in Fig. 3(b) as the average of three repeated experiments with the error bars representing the variation of the measured value. As the index of refraction of the liquid is increased a linear shift of the resonance position to longer wavelengths is detected. A shift of 50 nm is recorded for a change in the index of refraction of the liquid of $\Delta n = 0.3$. This results in a sensitivity of 6×10^{-3} , which is slightly higher than that for the photonic band gap measurement.

In conclusion, we have demonstrated the concept of applying 3D photonic crystals to detecting changes of refractive index in a microfluidic device. The 3D photonic crystals were integrated into a microfluidic device using femtosecond direct laser fabrication of the photonic crystals and microfluidic channels. Shifts in the photonic band gap and defect resonance positions as a result of a change in the refractive index of the liquid in the microfluidic channel are measured with Fourier transform infrared spectroscopy. A change of 6×10^{-3} in the refractive index can be detected using the photonic crystal with planar defect. This method of sensing changes in refractive index is able to measure both a relative shift in the refractive index and the absolute value of the refractive index as a function of the band gap position.

The authors would like to thank the Australian Research Council for its support.

¹M. A. Cooper, Nat. Rev. Drug Discovery **1**, 515 (2002).

²C. Monat, P. Domachuck, and B. Eggleton, Nat. Photonics **1**, 106 (2007).

³C. J. Choi and B. T. Cunningham, Lab Chip **6**, 1373 (2006).

⁴B. Cunningham, P. Li, B. Lin, and J. Pepper, Sens. Actuators B **81**, 316 (2002).

⁵D. Erickson, T. Rockwood, T. Emery, A. Scherer, and D. Psaltis, Opt. Lett. **31**, 59 (2006).

⁶H. J. Kima, S. Kima, H. Jeon, J. Ma, S. H. Choi, S. Lee, C. Ko, and W. Park, Sens. Actuators B **124**, 147 (2007).

⁷M. J. Ventura, M. Straub, and M. Gu, Appl. Phys. Lett. **82**, 1649 (2003).

⁸M. J. Ventura, M. Straub, and M. Gu, Opt. Express **13**, 2767 (2005).

⁹M. Straub, M. J. Ventura, and M. Gu, Phys. Rev. Lett. **91**, 043901 (2003).